



# Analysis of micro-rods machined using reverse micro-EDM

Amit Kumar Singh<sup>1</sup> · Promod Kumar Patowari<sup>2</sup> · Nishikant V. Deshpande<sup>2</sup>

Received: 17 June 2018 / Accepted: 30 November 2018 / Published online: 7 December 2018  
© The Brazilian Society of Mechanical Sciences and Engineering 2018

## Abstract

In today's world, microstructures have a wide range of applications in the field of biomedical devices, aerospace engineering, MEMS device elements, etc. In the recent years, reverse micro-electro-discharge machining (R- $\mu$ EDM) has evolved from  $\mu$ EDM that has become one of the promising technologies to fabricate precise components and microstructures of various shapes with high aspect ratio. In this work, micro-tools (rods) of average size (diameter) 182  $\mu\text{m}$  have been machined using copper sheet from bulk tungsten rod of 800  $\mu\text{m}$  diameter by R- $\mu$ EDM process. Moreover, Taguchi's *L16* orthogonal array has also been applied for designing the experiments. Feed rate, capacitance and voltage are considered as the parameters of the process. The response parameters such as machining time, erosion rate and dimensional variation have been analyzed in detail for different combinations of the process parameters. It is a well-known fact that the tool wear is the main culprit and responsible for the error in the micro-rods. Dimensional error has been quantified over the entire length of the micro-rods through the measurement process, and the minimum standard deviation is found to be 1.13  $\mu\text{m}$  at a feed rate of 5  $\mu\text{m/s}$ , capacitance of 1000 pF and voltage of 120 V. Further, machining data have been collected in real time and the behavior of machining time with work feed has been studied. In addition to it, a simple analytical model has been developed for calculating the erosion rate and it is seen that voltage produces more effect on erosion rate and machining time than the other parameters. Additionally, using the feed rate, capacitance and voltage at which minimum deviation took place, an array of  $4 \times 4$ , i.e., 16 micro-rods with 58  $\mu\text{m}$  diameter and 830  $\mu\text{m}$  length, has been fabricated on the bulk tungsten rod of 800  $\mu\text{m}$  diameter.

**Keywords** Micro-machining · Discharge · Reverse · Electrical · EDM · Taguchi

## 1 Introduction

Microstructure fabrication uses micro-machining technology having distinctive advantages, e.g., require less material and energy, as well as occupying minimum space. Micro-tools are widely used for machining of micro-parts and components with various shapes using conventional and non-conventional processes, for instance, micro-drilling, micro-punching, micro-milling [1–8].

One of the promising methods of fabricating microstructures is micro-electrical discharge machining ( $\mu$ EDM). The

basic mechanism of this technique is same as EDM. This process utilizes sequential electrical spark energy in pulse form in between the tool and the workpiece, while both are deep in the dielectric fluids like kerosene, hydrocarbon oil, deionized water [9]. It can be used to machine materials which are electrically conductive irrespective of their hardness. However, in this process, erosion rate is not as fast as conventional EDM due to the small pulse energy involved during the machining process. From the last decade, one of the variants of  $\mu$ EDM which is known as reverse  $\mu$ EDM (R- $\mu$ EDM) has been gaining popularity for the fabrication of single- as well as multiple-tipped micro-rod of various shapes with high aspect ratio [10–16]. Multiple-tipped micro-rods have a plenty of applications in industries such as drilling of micro-holes in probe card for testing semiconductor device and perforated shadow mask with various shapes which are used in CRT monitors. Tungsten micro-rods are also widely used in the form of array in medical science for capturing the neural signals of the animal species, where the diameter of the micro-rod varies from 25 to 50  $\mu\text{m}$  [17,

---

Technical Editor: Márcio Bacci da Silva, Ph.D.

✉ Amit Kumar Singh  
amit.kumar965@yahoo.com; amit.kumar996@gmail.com

<sup>1</sup> Department of Mechanical Engineering, National Institute of Technology Mizoram, Aizawl, Mizoram 796012, India

<sup>2</sup> Department of Mechanical Engineering, National Institute of Technology, Silchar, Assam, India

18]. Moreover, it is also used with the diameter of the order of 50–100  $\mu\text{m}$  as a tip in thickness profilometer for contact mode. It is also used as a micro-probe for electrical measurement. In the present work, copper plate electrode is used as a tool electrode because it possesses desirable properties like relatively low wear rate and easily machinable which is very essential for stable machining [19, 20].

From the existing literature, it is seen that few researchers have contributed toward understanding of the R- $\mu\text{EDM}$  process. Some of the foremost studies which have made a reasonable contribution in the field of R- $\mu\text{EDM}$  have been discussed in this section. Kim et al. [11] worked on R- $\mu\text{EDM}$  process and fabricated micro-rods and multiple electrodes with various shapes. They investigated the machining characteristics of the R- $\mu\text{EDM}$  under varying capacitances and applied voltages. They also investigated the wear ratio. Mastud et al. [21] fabricated micro-electrode arrays with different cross sections and dimensions. Geometrical accuracy, surface finish and surface morphology were assessed on machined micro-electrodes. Moreover, micro-electrode of 60  $\mu\text{m}$  diameter was fabricated successfully with an aspect ratio of 33. Mujumdar et al. [22] conducted an experimentation using *L8* orthogonal array for making a micro-rod array of high aspect ratio in order to understand the consequences of different input parameters like feed rate, threshold voltage, capacitance and gap voltage on the response parameters like zero error length, dimensional accuracy, and surface roughness. They observed that in comparison with other process parameters, the influence of gap voltage is more on the exactness of micro-rods in almost every position. Investigation of surface morphology disclosed that the presence of micro-craters on the tip surface makes it less smooth compared to the root surface. They showed that chemical composition affects significantly over the whole length of the micro-rod. Debris gathering within the inter-electrode gap in R-MEDM is a major problem. Mastud et al. [23] used vibration-assisted R-MEDM to avoid debris accumulation, and the consequent improvement in machining process enabled the creation of textured/engineered surfaces. For that, simulation was performed with the effect of electrode vibrations using quantified debris particles with ejection velocity, numbers, and estimated sizes and the result highlighted that oscillatory motion was created due to the electrode vibrations within the dielectric fluid and debris particles. The reciprocating motion of the debris particles and the flow reversal of the dielectric fluid improve the overall process stability, which was totally absent in case of inter-electrode gap which is in a fixed condition (in case of without vibration-assisted). Singh et al. [16] have contributed some work on R- $\mu\text{EDM}$ , in which they discussed the machining of straight and target length of micro-rod. They machined a straight micro-rod with a target length of 1 mm. They also fabricated [10] multiple-tipped micro-rod simultaneously on

bulk rod and discussed the TWR and MRR. Talla et al. [12] have used EDM in reverse polarity to fabricate the arrayed structures on mild steel; for that, they have designed the experimental run through the statistical approaches such as response surface methodology (RSM). They obtained the optimal parametric condition using principal component analysis (PCA)-based gray relational analysis (GRA) and ensured it by performing the confirmation test. Micro-tool electrodes with  $3 \times 3$  array are fabricated through combined actions of WEDG, R- $\mu\text{EDM}$  and electrodes' end trimming. Further, the same method is used to machine  $3 \times 3$  array of hexagonal micro-cavities where hump of debris is accumulated at the electrodes' tip that are removed using oil dielectric [13].

Based on the studies which have been discussed above, it is evident that dimensional analysis, machining time and erosion rate have not been explored much by researchers while machining micro-rod by reverse  $\mu\text{EDM}$  process. Authors have indicated that the tool wear is the main culprit and responsible for the error in the micro-rods. In this work, dimensional errors have been quantified over the entire length of the micro-rods through the measurement process in which error percentage in diameter and standard deviation have been calculated along the machined surface in detail. Further, machining data have been collected during the machining process in real time and the behavior of the machining time with the work feed has been studied in which the reasons have been detailed, how the machining time is drastically increased/decreased while machining with different parametric conditions. Moreover, a simple analytical model has been developed for calculating the erosion rate. Then after, the proper reason for decreasing the erosion rate with the machining progresses gradually has been presented. Additionally, an array of  $4 \times 4$ , i.e., 16 micro-rods, has been fabricated simultaneously on bulk rod of tungsten. In the present work, micro-rod is fabricated on bulk tungsten rod at different levels of input parameters such as feed rate, capacitance and voltage in order to characterize the reverse  $\mu\text{EDM}$  process such as machining time, erosion rate and dimensional variation.

## 2 Experimentation

In the present work, experiments have been carried out on  $\mu\text{EDM}$  machine (Sinergy nano systems, Navi Mumbai-400705, Model Type: Hyper-15) that has an accuracy of  $\pm 5$  micron for the entire range in all axes and repeatability of  $\pm 1$  micron for all axes. The schematic diagram of experimental setup is shown in Fig. 1. Hydrocarbon oil has been used as dielectric fluid because it possesses properties such as high dielectric strength, less possible time to breakdown and high degree of fluidity [20]. Moreover, tungsten bulk rod

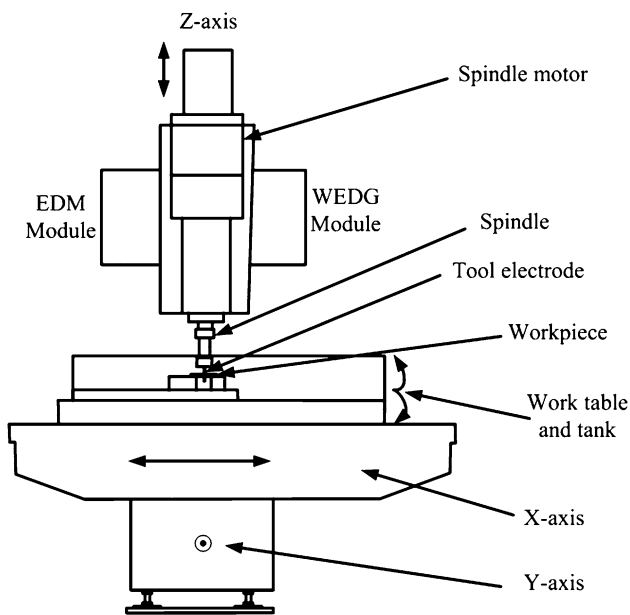


**Fig. 1** Schematic diagram of the experimental setup

having 800  $\mu\text{m}$  diameter has been used as a workpiece and copper thin plate having thickness 293  $\mu\text{m}$  with pre-drilled hole of diameter 212  $\mu\text{m}$  has been selected as tool electrode.

Experimental conditions have been divided into two parts, i.e., fixed parameters and control parameters with its level. The control parameters include feed rate, capacitance and voltage, whereas fixed parameters include workpiece and tool electrode material, and dielectric fluid. Kim et al. have highlighted that at 100 V, tungsten carbide was machined stably [11]. Hence, voltage of four levels has been selected for the experimentation, out of which two levels of voltage are above 100 V and one below it. Moreover, the machine in which experiments are conducted is capable of operating with a capacitance of 33 pF, 100 pF, 1000 pF and 10,000 pF and it is explained by the authors that a capacitance of 33 pF and 10,000 pF results in unfavorable machining of bulk tungsten rod and the reasons of which are highlighted by Singh et al. [24]. Therefore, two levels of capacitance, i.e., 100 pF and 1000 pF, are selected for the experimentation. Further, four levels of feed rate have been used with an interval of five micrometers per second starting from a slow feed rate of 5  $\mu\text{m}/\text{s}$  to a faster feed rate of 20  $\mu\text{m}/\text{s}$ . Experimentation has been performed using Taguchi's *L16* orthogonal array. The reason for using Taguchi methodology is that it determines the significant factor which directly influences output parameters of the machining process in the least number of experimentations [25–30]. The detailed results are presented in Table 1.

For the initialization of the R- $\mu\text{EDM}$  process, micro-tool is fabricated as shown in Fig. 2, by block electrical discharging grinding (BEDG) process at the voltage of

**Table 1** *L16* orthogonal array of Taguchi design

Exp. nos.	Voltage (V)	Feed rate ( $\mu\text{m}/\text{s}$ )	Capacitance (pF)	Erosion rate ( $10^{-5} \mu\text{m}^3/\text{min}$ )
1	80	5	100	5.256
2	80	10	100	6.950
3	80	15	1000	17.448
4	80	20	1000	17.143
5	100	5	100	11.597
6	100	10	100	13.499
7	100	15	1000	30.466
8	100	20	1000	41.998
9	120	5	1000	76.092
10	120	10	1000	66.471
11	120	15	100	147.604
12	120	20	100	73.300
13	140	5	1000	85.086
14	140	10	1000	149.621
15	140	15	100	334.884
16	140	20	100	315.081

100 V, capacitance of 100 pF, feed rate of 10  $\mu\text{m}/\text{s}$  and spindle speed of 1000 rpm. The micro-rod machined by BEDG process is further utilized for making multiple numbers of holes on the plate electrode. Later, the plate electrode having multiple numbers of holes is used as a tool in R- $\mu\text{EDM}$  process. Each of the holes on the plate electrode is utilized for fabricating a single micro-rod. For machining a micro-rod, the tungsten bulk rod is made to move 1 mm into the tool electrode. The advantage of this technique is that an array of micro-rods can be fabricated simultaneously on a bulk rod. The process mechanism of R- $\mu\text{EDM}$  for the machining of micro-rods is illustrated in Fig. 3.

### 3 Results and discussion

The scanning electron microscope (SEM) micrographs of the fabricated micro-rods are shown in Fig. 4 and are machined based on Taguchi's *L16* orthogonal array. A thorough experimental examination is conducted by altering the different process parameters like feed rate, capacitance and voltage in order to detect their effect on output parameters like dimensional variation, machining time ( $t$ ) and erosion rate (ER).

#### 3.1 Study of dimensional variation

Dimensional variation is the measure of the variation in diameter of the micro-rod over the machined length. For

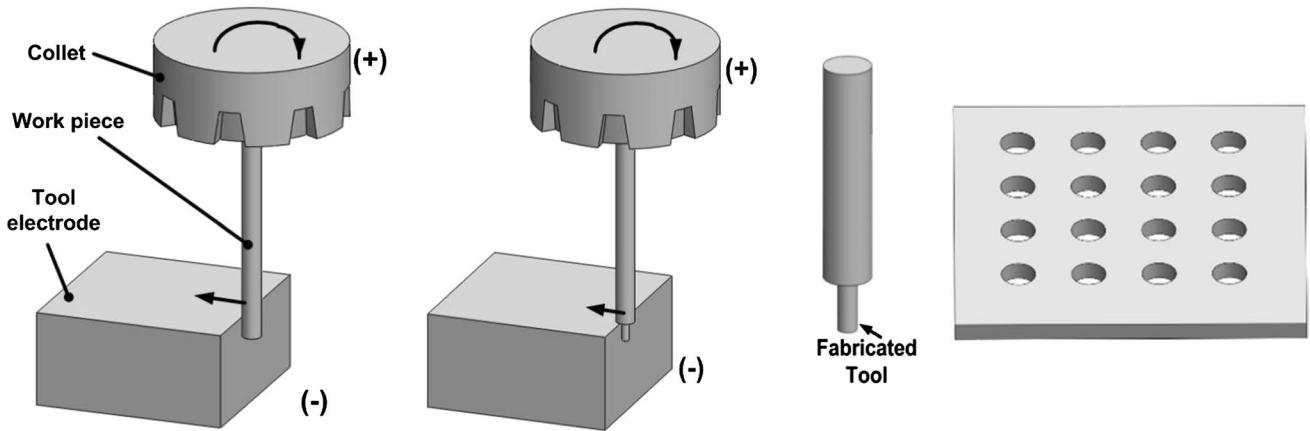


Fig. 2 Preparation of micro-rod for R-μEDM using BEDG process

Fig. 3 Schematic diagram of the fabrication of micro-rod using R-μEDM process

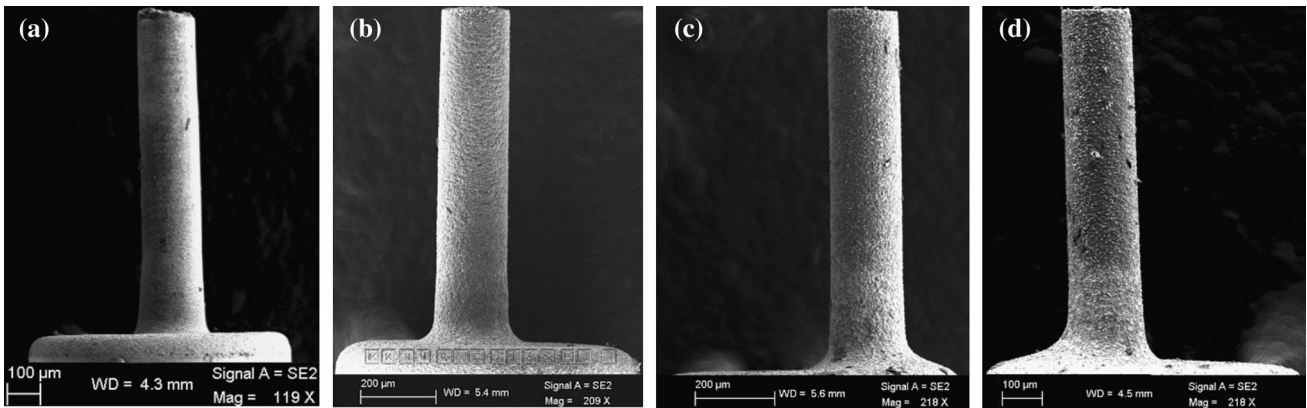
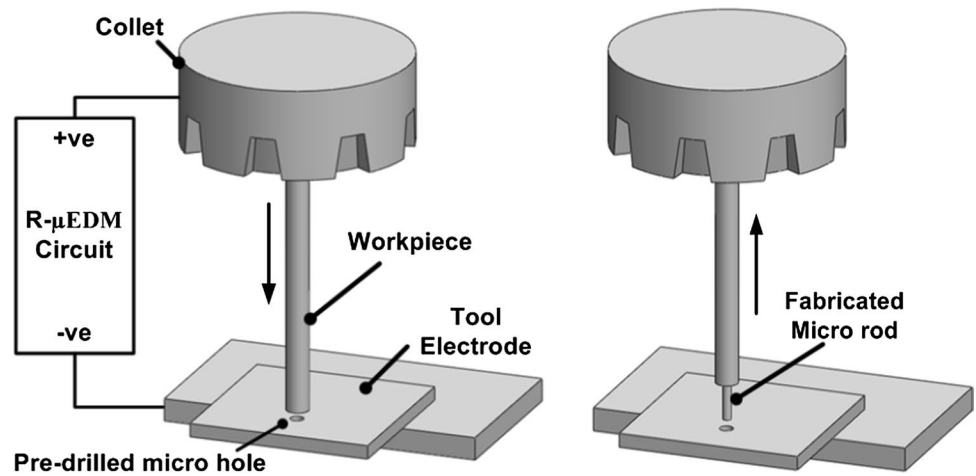
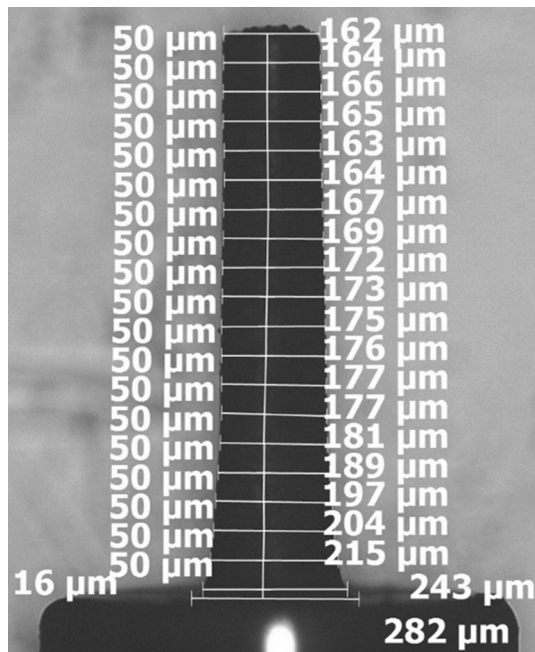


Fig. 4 Images of SEM machined at a 80 V, 5 μm/s, 100 pF b 80 V, 20 μm/s, 1000 pF c 120 V, 10 μm/s, 1000 pF d 140 V, 10 μm/s, 1000 pF

performing the analysis, the diameter of the machined micro-rod is measured lengthwise at 20 distinct points as shown in Fig. 5. The measurement is carried out from the

tip of the machined micro-rod till its root and each of the consecutive distinct points are separated by 50 μm excluding the last point.



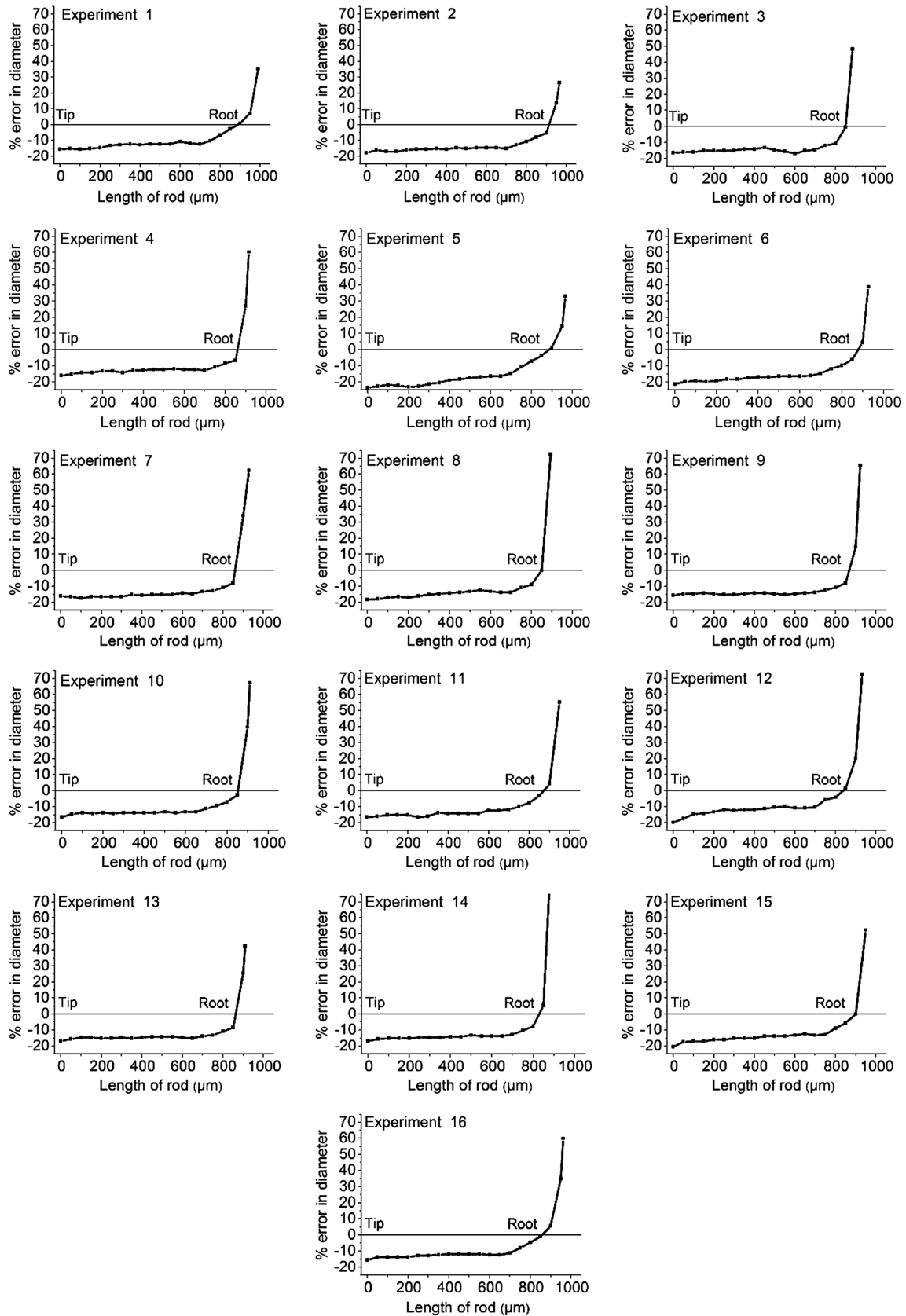


Fig. 6 Percentage deviation in diameter along the length of the micro-tool for all parametric conditions

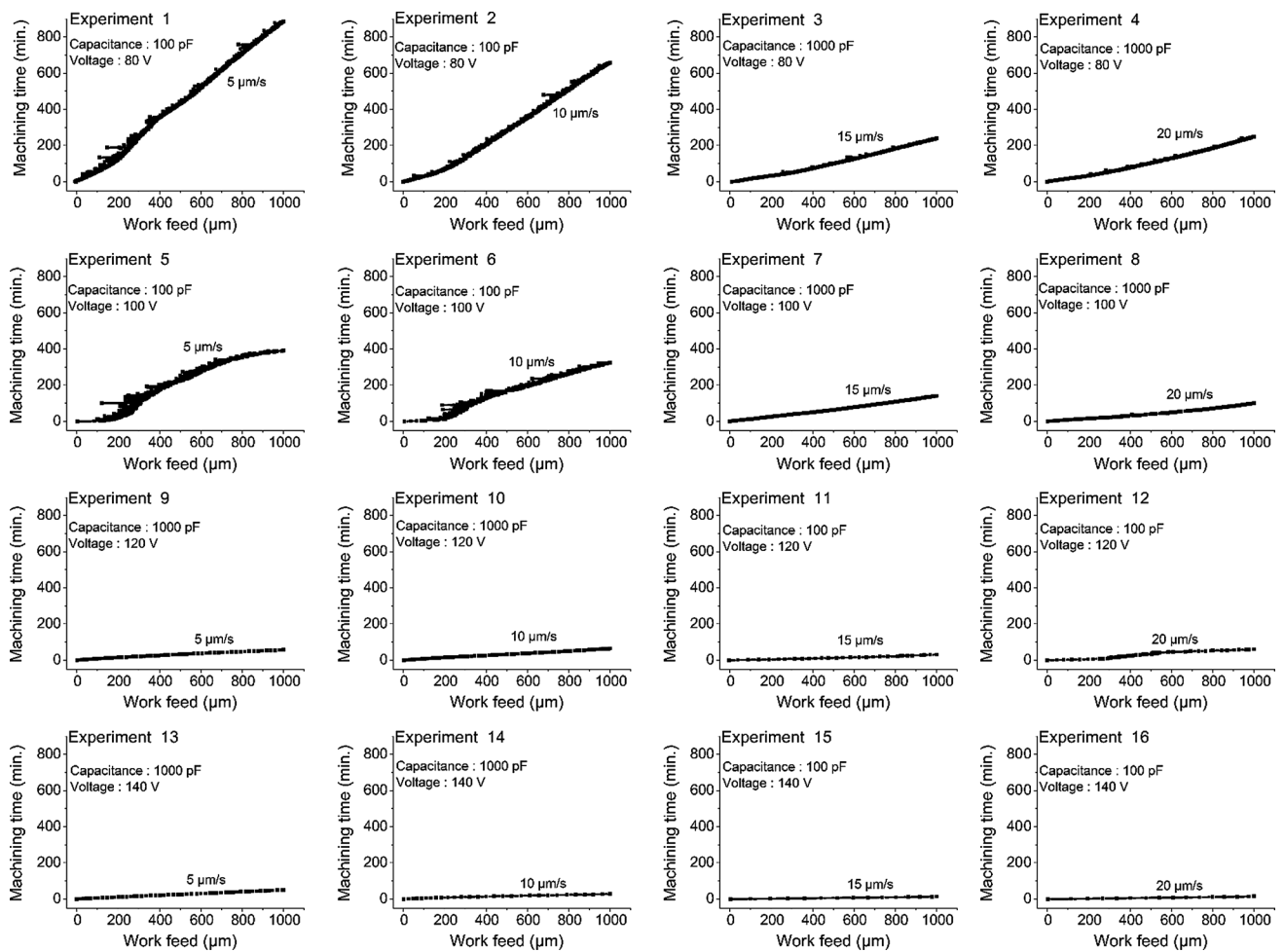


Fig. 7 Plot between work feed and machining time for all parametric conditions

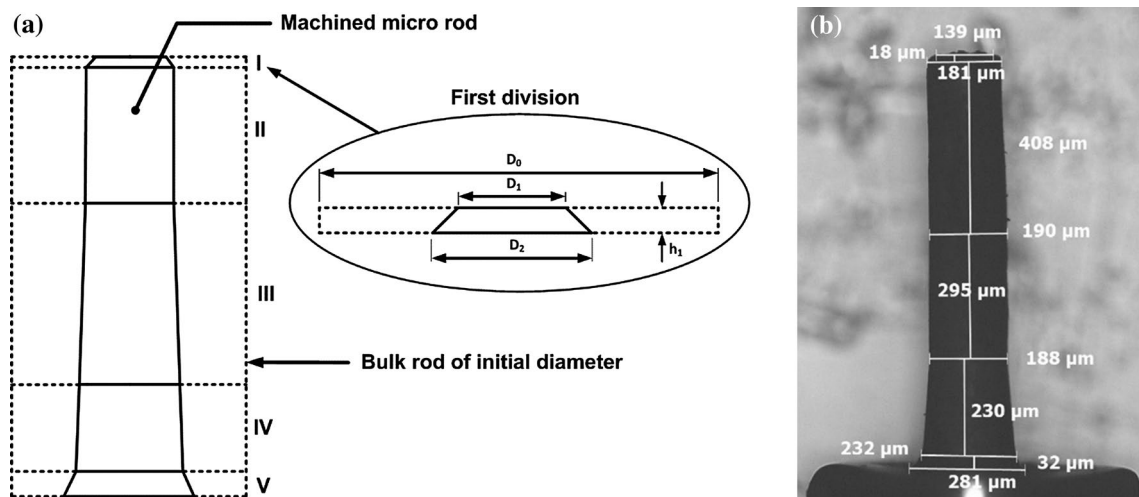


Fig. 8 a Schematic diagram of the fabricated micro-tool and its enlarged view of the first division. b Real view of fabricated micro-tool

Using the equation, erosion rate has been calculated, where the number of divisions ( $n$ ) is taken as five. Equation (1) is valid for all the experimental conditions (experimental run) except the number of divisions mentioned in that equation, which is different for different parametric conditions. Subsequently, erosion rate has been calculated for each experimental run.

$$\text{Erosion rate} = \sum_{i=1}^5 \frac{\pi h_i (3D_0 - D_i^2 - D_{i+1}^2 - D_i D_{i+1})}{12 t_i} \quad (1)$$

where  $i$  varies from 1 to 5 and it represents the number of divisions for the machined micro-rod,  $D_0$  is the original diameter of the workpiece material,  $D_i$  and  $D_{i+1}$  are the top and bottom diameters of particular division of the fabricated machined micro-rod, and  $h_i$  and  $t_i$  are the corresponding thickness and machining time of the machined micro-rod, respectively.

Figure 9 shows the average effect of parameters such as voltage (V), feed rate ( $\mu\text{m/s}$ ) and capacitance (pF) on erosion rate. The plot of the average effect of voltage vs erosion rate highlights that the rate of erosion rises upon increasing the voltage. The reason for it is that the spark gap between the electrodes rises up with the rise in the levels of voltage, and this allows effective flushing of debris particles. This leads to improvement in the erosion rate. It is also seen from the main effect plot that the erosion rate rises up with the rise in

the feed rate to some extent, and later, it starts to decrease. It is known that on varying feed rate, the machining time also varies. Faster feed rate results in lower machining time, and this is because the workpiece moves toward the tool surface at a greater speed. But, at the same time, there is a frequent contact between the surfaces of the electrodes and so the electrodes experience arcing at higher feed rate compared with lower feed rate, thus resulting in reduction of the erosion rate.

The main plot (Fig. 9) highlights that the erosion rate is lower at a capacitance of larger value compared with capacitance of lower value. It can be realized from Fig. 10a and b that the machined micro-rod length achieved at 1000 pF, i.e.,  $y_2 (= 1 - y_1)$ , is smaller compared with the micro-rod length attained at 100 pF, i.e.,  $x_2 (= 1 - x_1)$ . It is due to the reason that tool wear is found more at 1000 pF during the experimentation and due to this deeper recess is created on the tool plate. The recess is occupied by the length of un-machined bulk rod. The length of the un-machined bulk rod, i.e.,  $x_1$  at 100 pF, is smaller compared with  $y_1$  at 1000 pF as shown in Fig. 10. This is the reason for getting lower erosion rate at higher capacitance value. From ANOVA (as shown in Table 2), it can also be realized that voltage contributes a greater percentage toward erosion rate and subsequently contributed to the control parameters like feed rate and capacitance.

Figure 11 indicates the effect of erosion rate at different zones along the micro-rod's length, where the first

Fig. 9 Average effect of parameters on erosion rate at different levels

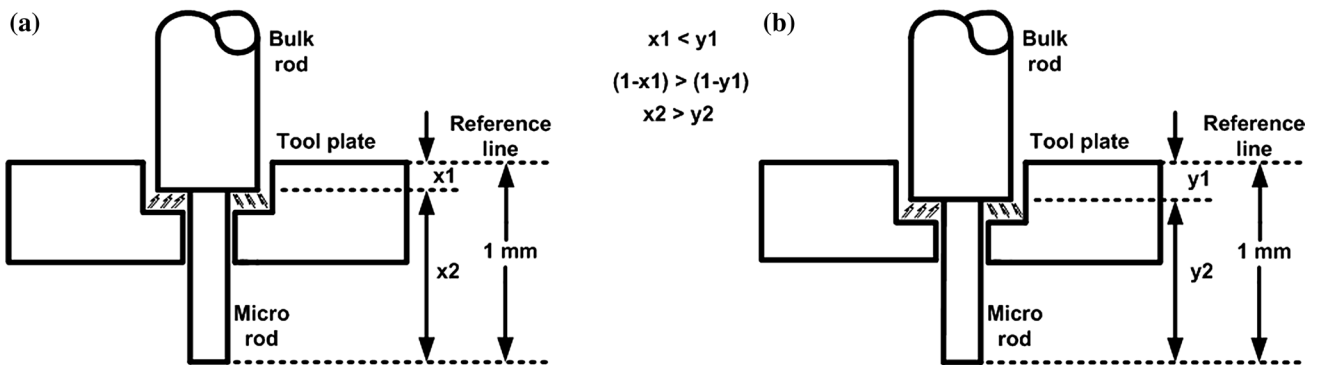
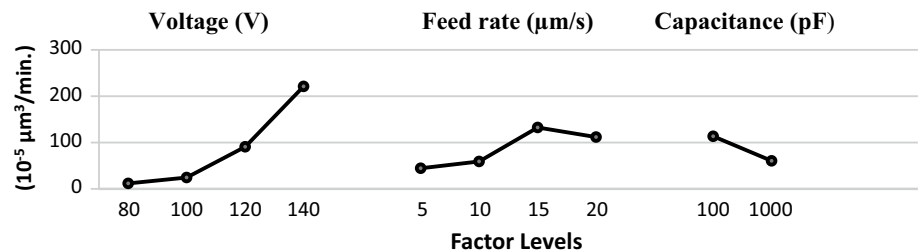
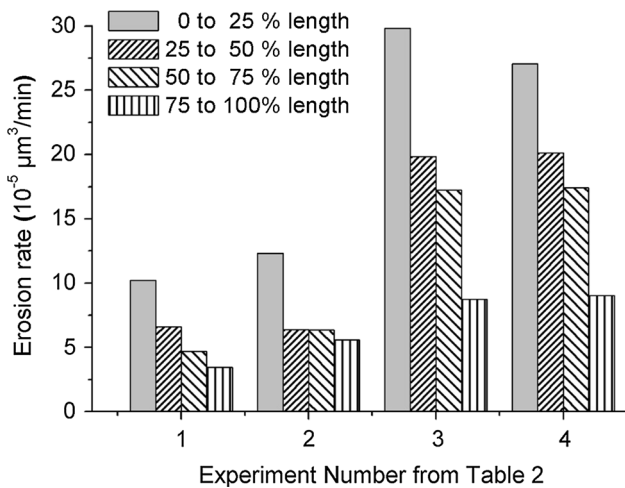


Fig. 10 Mechanism involved during the machining process (a) at 100 pF (b) at 1000 pF



**Table 2** ANOVA for erosion rate

Parameter	DOF ( <i>f</i> )	Sum of sqrs. ( <i>S</i> )	Variance ( <i>V</i> )	<i>F</i> -ratio ( <i>F</i> )	Pure sum ( <i>S'</i> )	Percent <i>P</i> (%)
Voltage	3	110,424.472	36,808.157	16.236	103,623.601	64.398
Feed rate	3	21,121.916	7040.638	3.105	14,321.045	8.9
Capacitance	1	11,227.715	11,227.715	4.952	8960.758	5.568
Other/error	8	18,135.655	2266.956			21.134
Total	15	160,909.761				100.00

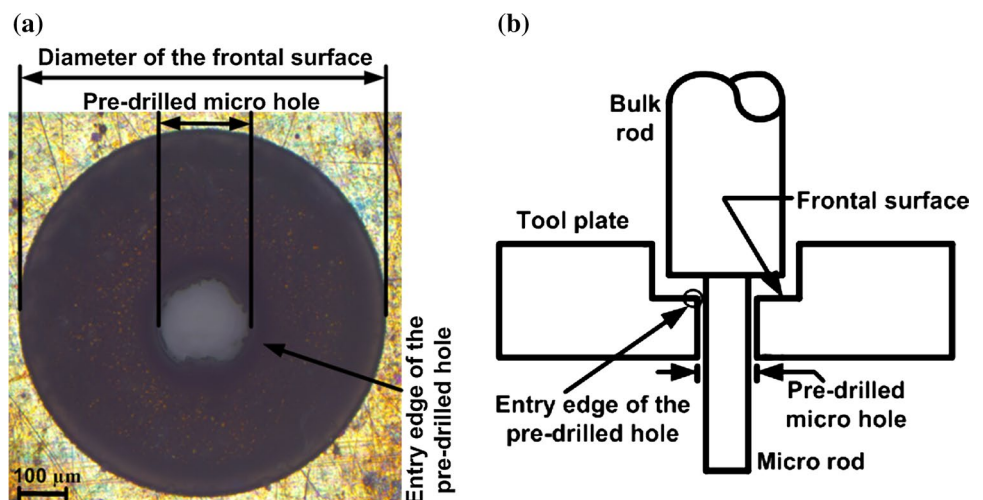


**Fig. 11** Effect of erosion rate on different zone lengths

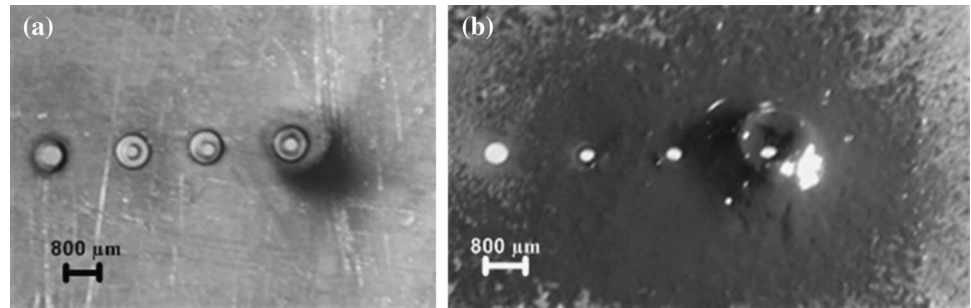
zone is the zone which extends from the tip (0% of the length) to 25% of length, followed by 25–50%, 50–75% and 75–100% of the length. It is observed from Fig. 11 that the rate of erosion reduces with the rise in the length of the machined workpiece. This is because of the fact that as the machining advances, tool wear takes place, and this rises continuously by taking the material progressively from the frontal surface, entry edge of the pre-drilled hole and pre-drilled micro-hole of the tool electrode as shown in

Fig. 12. The effect of the tool wear is seen in the machined micro-rod in the form of un-machined length, i.e.,  $x_1$  and  $y_1$ , as shown in Fig. 10. Moreover, the effect of tool wear has also been seen on machined micro-rod in the form of tapered shape which is from tip to roots as shown in Figs. 6 and 8. Hence, the amount of material removed from the workpiece is decreasing as the machining advances from first zone (i.e., 0–25% of length) followed by 50 to 75% and 75 to 100% of length. One more observation seen during the machining process is that the machining time increases with the increase in the advancement of the process, even though the amount of material removed from the workpiece is decreasing with time. This is because the debris particles adhere at the rear surface of the copper plate electrode as shown in Fig. 13. This phenomenon of adhesion of the debris particles gradually increases as workpiece advances. It obstructs the process progressively with time during the machining process, thus increasing the machining time. The decreasing effect of material removal from the workpiece is more prominent compared with the decreasing effect of machining time. The above-discussed explanation clarifies the reason of why erosion rate decreases during the machining of micro-rod from tip to root, i.e., from the first zone (i.e., 0–25% of length) followed by 50–75% and 75–100% of length.

**Fig. 12** a Condition of tool plate after machining of micro-rod, showing the pre-drilled hole and worn out frontal surface. b Schematic representation of workpiece and tool plate, showing pre-drilled, worn out of the tool and the fabricated micro-rod



**Fig. 13** Copper tool electrode plate with **a** front surface **b** rear surface



#### 4 Machining of arrayed micro-rods

In the first part of the work, micro-rods with single tip have been machined successfully and subsequently obtained the parametric condition in which straight micro-rods have been fabricated, where voltage of 120 V, feed rate of 5  $\mu\text{m/s}$  and capacitance of 1000 pF have been used. In the second part of the work, a straight and very high aspect ratio micro-rod (aspect ratio 62) has been fabricated on a bulk rod of tungsten using BEDG process. This micro-rod has been used to drill multiple numbers of holes in the tool plate. Afterward, micro-rods with multiple tips/array of micro-rods have been fabricated on the bulk rod of tungsten as indicated in Fig. 14. It has been fabricated by using the same parametric condition (voltage of 120 V, feed rate of 5  $\mu\text{m/s}$  and capacitance of 1000 pF) which is mentioned in the first part of the work.

Initially, in the study, a straight and very high aspect ratio micro-rod is generated with an aspect ratio of 62 by means of BEDG process on a bulk tungsten rod of initial diameter 500  $\mu\text{m}$  at a feed rate of 10  $\mu\text{m/s}$ , capacitance of 1000 pF and voltage of 100 V. The micro-rod thus produced has an average diameter of 55  $\mu\text{m}$  as shown in Fig. 14a. Using this micro-rod, an array of 4 $\times$ 4, i.e., 16 micro-holes, with an average diameter of 80  $\mu\text{m}$  is drilled on a thin plate of thickness 300  $\mu\text{m}$  depicted in Fig. 14b. The array of micro-holes is utilized to produce an array of micro-rods on bulk rod of tungsten having 800  $\mu\text{m}$  by means of R- $\mu\text{EDM}$  process. Each of the fabricated micro-rods is 830  $\mu\text{m}$  long with a diameter of 58  $\mu\text{m}$  as shown in Fig. 14c. This process is accomplished at the feed rate of 5  $\mu\text{m/s}$ , capacitance of 1000 pF and voltage of 120 V, because at these parametric conditions minimum standard deviation is found while machining single micro-rod on the tungsten bulk electrode as discussed in Sect. 3.1. This shows that using this process an array of any polygon shape of micro-rods/micro-tool can be fabricated.

#### 5 Conclusions

An experimental study is performed by R- $\mu\text{EDM}$  process using *L16* Taguchi's methodology. Process parameters used in the experiments are feed rate, capacitance and voltage.

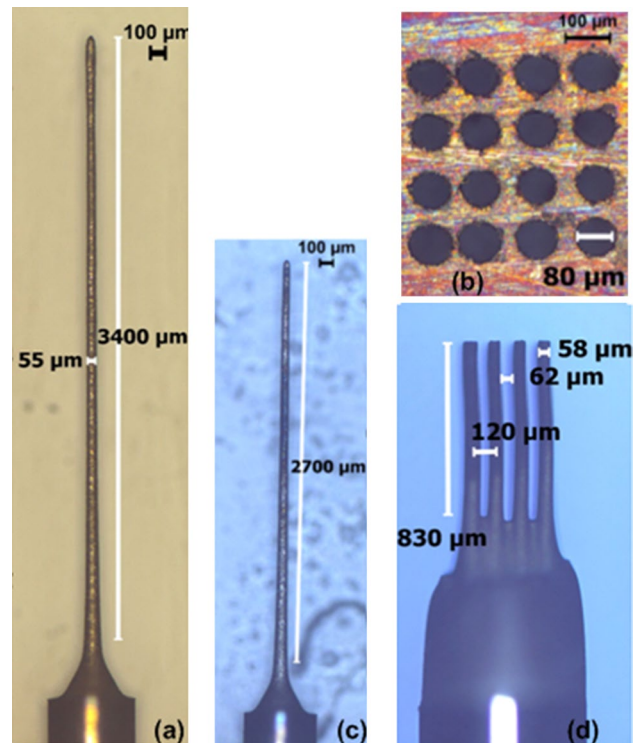


**Fig. 14** Machining of arrayed micro-tools on bulk rod using R- $\mu\text{EDM}$  process. **a** Circular micro-tool fabricated using BEDG process. **b** Array of micro-hole is drilling using fabricated micro-tool. **c** Condition of micro-tool after drilling micro-holes. **d** Fabricated arrayed micro-tools on tungsten rod

The effect of process parameters on response measures such as dimensional variation, machining time ( $t$ ) and erosion rate (ER) has been studied in this work. The study highlights the following specific conclusions:

1. Micro-rods with single tip have been fabricated, and subsequently, thorough experimental investigations have been performed to know the effect of different process parameters such as feed rate, capacitance and voltage on response parameters, for instance, dimensional variation, machining time ( $t$ ) and erosion rate (ER).
2. Afterward, the same technology has been adopted to fabricate micro-rods with multiple tips in a single run.

3. For dimensional variation, percentage of dimensional error in the tip surface diameter is greater than the middle surface diameter of the micro-rod. It is observed that the average error percentage at the tip is  $-17.7\%$ , at the middle of the rod is  $-13.9\%$ , and at the point which is located on 85% distance from the tip of the rod is  $-3.7\%$ . A minimum standard deviation of error% of diameter in the machined micro-rod is found to be 1.13 by considering 80% length on the machined micro-rod from its tip.
4. For machining time, it is observed that the time of machining reduces with the rise in capacitance from 100 to 1000 pF and with the increase in voltage from 80 to 140 V. Likewise, with the rise in feed rate from 5 to 20  $\mu\text{m/s}$ , machining time also decreases.
5. For erosion rate, it is seen that the rate of erosion rises with the rise in voltage from 80 to 140 V. It also increases with the rise in feed rate to some extent from a level of 5 to 15  $\mu\text{m/s}$ , but it starts to decrease when the feed rate is increased beyond 15  $\mu\text{m/s}$ . Rate of erosion is low at higher capacitance value of 1000 pF compared with capacitance at lower value, i.e., 100 pF.
6. It is also observed that the rate of erosion reduces with the rise in the length of the machined workpiece from first zone (i.e., 0–25% of length) followed by 50–75% and 75–100% of length.
7. In the second part of the work, an array of micro-rod is fabricated on bulk rod having 830  $\mu\text{m}$  length with 58  $\mu\text{m}$  diameter at the feed rate of 5  $\mu\text{m/s}$ , capacitance of 1000 pF and voltage of 120 V.

## Compliance with ethical standards

**Conflict of interest** The authors declare that they have no conflict of interest.

## References

1. Masuzawa T, Tönshoff HK (1997) Three-dimensional micromachining by machine tools. *CIRP Ann Manuf Technol* 46:621–628
2. Tamang SK, Natarajan N, Chandrasekaran M (2017) Optimization of EDM process in machining micro holes for improvement of hole quality. *J Braz Soc Mech Sci Eng* 39:1277–1287
3. Das AK, Kumar P, Sethi A et al (2016) Influence of process parameters on the surface integrity of micro-holes of SS304 obtained by micro-EDM. *J Braz Soc Mech Sci Eng* 38:2029–2037
4. Singh AK, Patowari PK, Deshpande NV (2013) Micro-hole drilling on thin sheet metals by micro-electro discharge machining. *J Manuf Technol Res* 5:137
5. Kar S, Patowari PK (2018) Electrode wear phenomenon and its compensation in micro electrical discharge milling: a review. *Mater Manuf Process* 33:1491–1517
6. Hourmand M, Sarhan AAD, Sayuti M (2017) Characterizing the effects of micro electrical discharge machining parameters on material removal rate during micro EDM drilling of tungsten carbide (WC-Co). In: IOP conference series: materials science and engineering. IOP Publishing, p 12005
7. Chavoshi SZ, Goel S, Morantz P (2017) Current trends and future of sequential micro-machining processes on a single machine tool. *Mater Des* 127:37–53
8. Mishra K, Mukhopadhyay P, Sarkar BR et al (2018) Improvement of micro-EDM performances with aid of vibration. *Int J Precis Technol* 8:38–65
9. Chakraborty S, Dey V, Ghosh SK (2015) A review on the use of dielectric fluids and their effects in electrical discharge machining characteristics. *Precis Eng* 40:1–6
10. Singh AK, Patowari PK, Deshpande NV (2017) Effect of tool wear on microrods fabrication using reverse  $\mu\text{EDM}$ . *Mater Manuf Process* 32:286–293
11. Kim BH, Park BJ, Chu CN (2006) Fabrication of multiple electrodes by reverse EDM and their application in micro ECM. *J Micromech Microeng* 16:843
12. Talla G, Gangopadhyay S, Kona NB (2017) Experimental investigation and optimization during the fabrication of arrayed structures using reverse EDM. *Mater Manuf Process* 32:958–969
13. Tong H, Li Y, Zhang L (2018) Servo scanning 3D micro EDM for array micro cavities using on-machine fabricated tool electrodes. *J Micromech Microeng* 28:25013
14. Gao S, Huang H (2017) Recent advances in micro-and nanomachining technologies. *Front Mech Eng* 12:18–32
15. Hourmand M, Sarhan AAD, Sayuti M (2017) Micro-electrode fabrication processes for micro-EDM drilling and milling: a state-of-the-art review. *Int J Adv Manuf Technol* 91:1023–1056
16. Singh AK, Patowari PK, Deshpande NV (2016) Experimental analysis of reverse micro-EDM for machining microtool. *Mater Manuf Process* 31:530–540
17. Nicolelis MAL (2010) *Methods for neural ensemble recordings*. CRC Press, Boca Raton
18. Tathireddy P, Rakwal D, Bamberg E, Solzbacher F (2009) Fabrication of 3-dimensional silicon microelectrode arrays using micro electro discharge machining for neural applications. In: Solid-state sensors, actuators and microsystems conference, 2009. TRANSDUCERS 2009. International. IEEE, pp 1206–1209
19. Amorim FL, Weingaertner WL (2007) The behavior of graphite and copper electrodes on the finish die-sinking electrical discharge machining (EDM) of AISI P20 tool steel. *J Braz Soc Mech Sci Eng* 29:366–371
20. Jain VK (2009) *Advanced machining processes*. Allied Publishers, New Delhi
21. Mastud SA, Singh RK, Joshi SS (2009) Investigation of reverse micro-EDM process for generating high aspect ratio micro-electrode arrays. Professional Engineering Publishing Ltd, London
22. Mujumdar SS, Mastud SA, Singh RK, Joshi SS (2010) Experimental characterization of the reverse micro-electrodischarge machining process for fabrication of high-aspect-ratio micro-rod arrays. *Proc Inst Mech Eng Part B J Eng Manuf* 224:777–794
23. Mastud SA, Kothari NS, Singh RK, Joshi SS (2015) Modeling debris motion in vibration assisted reverse micro electrical discharge machining process (R-MEDM). *J Microelectromech Syst* 24:661–676
24. Singh AK, Patowari PK, Deshpande NV (2013) Fabrication of micro tool using reverse-micro EDM. In: International conference on precision, meso, micro and nano engineering (COPEN-8: 2013). NIT Calicut, India, pp 218–221
25. Roy RK (2001) *Design of experiments using the Taguchi approach: 16 steps to product and process improvement*. Wiley, New York
26. Wangikar SS, Patowari PK, Misra RD (2017) Effect of process parameters and optimization for photochemical machining of brass and german silver. *Mater Manuf Process* 32:1747–1755

27. Gul M, Shah AN, Jamal Y, Masood I (2016) Multi-variable optimization of diesel engine fuelled with biodiesel using grey-Taguchi method. *J Braz Soc Mech Sci Eng* 38:621–632
28. Abhishek K, Datta S, Biswal BB, Mahapatra SS (2017) Machining performance optimization for electro-discharge machining of Inconel 601, 625, 718 and 825: an integrated optimization route combining satisfaction function, fuzzy inference system and Taguchi approach. *J Braz Soc Mech Sci Eng* 39:3499–3527
29. Khazaali H, Fereshteh-Saniee F (2018) Application of the Taguchi method for efficient studying of elevated-temperature incremental forming of a titanium alloy. *J Braz Soc Mech Sci Eng* 40:43
30. Gadhane ND, Gawande SH (2018) Optimizing performance of the *Jatropha* biodiesel engine using Taguchi approach. *J Braz Soc Mech Sci Eng* 40:235